BEM SIMULATIONS OF DIFFRACTION-OPTIMIZED GEOMETRICAL NOISE BARRIERS, WITH A FOCUS ON TUNABILITY

Sara Gasparoni[1], Paul Reiter[1,2], Reinhard Wehr[1], Marco Conter[1] and Manfred Haider[1]
[1] AIT, Austrian Institute of Technology, Vienna, Austria
[2] Technical University of Vienna, Vienna, Austria
sara.gasparoni@ait.ac.at

Traffic noise is an increasingly important problem with the increase in traffic volume. To counteract this, noise barriers are the most used traffic-noise-abatement tool. In an attempt to reduce the amount of material, and thus the costs for the construction of noise barriers, it is of interest to reduce the height of the barriers. One possibility to reduce the height is to use absorbing materials. This is a good solution but the porosity of these materials makes them very sensitive to clogging by dirt and changes their absorbance and their performance with time. In this paper, non-standard geometrical forms of noise barriers with added devices are investigated. The boundary element method is used to investigate the insertion loss produced by these noise barriers. This method is also used to propose tunable barriers that could adapt to the changing noise spectrum.

INTRODUCTION

Traffic noise is increasing with the increase in traffic volume. There are different methods that can be used to reduce traffic noise, for example traffic noise could be reduced at the source by producing low-noise asphalts or low-noise tyres, or at the receiver by using sound-absorbing materials for buildings. Noise barriers are a common way to shield residential areas from traffic noise, mainly because they can be built *ad hoc* after the problem of traffic noise has shown up.

While the efficiency in noise absorption can be evaluated experimentally with reverberation room and situ methods [1-3], simulations are a helpful and cost-saving tool in predicting and planning new noise barrier solutions. The boundary element method (BEM) has long been used in the simulation of noise barriers, as it proves to be an effective method whose results are compatible both with analytical solutions and experimental results [4]. Non-standard shapes of the barrier tops have been used to obtain a better performance of the barrier [5-10].

This paper uses a BEM simulation to study non-standard barrier shapes with a particular focus on the formation of a virtual soft plane for some frequencies. Destructive diffraction from the top edge of the barrier is used in order to optimize the shielding effect of the barrier. After verifying the effectiveness of alternative shapes, the possibility of tuning the barrier in frequency is examined. This is an interesting novel theme to be explored as it may give the opportunity to adapt the barrier to a changing noise environment.

BARRIER NUMERICAL MODEL

Perfectly reflecting (acoustically hard) materials are not considered the best choice for noise barriers, as they generate many unwanted reflections. Absorbing materials seem much more appropriate, but their impedance changes rapidly with time in the presence of dirt, which is in the case of highways. Different geometrical shapes have been used to obtain a specific input impedance for improved performance [5-7].

Consider the fork-shaped barrier shown in Figure 1(b). If the surfaces are rigid, the specific input impedance at the open side can be approximated by [5]

$$Z_{in} = i \cot(kd) \tag{1}$$

where d is the depth of the fork and k is the wavenumber. According to this equation, at frequencies f_n with $k_n d = (2n+1)\pi/2$, the impedance is zero. This means that for the range close to those frequencies, the fork element plays the role of a soft plane with complete absorbance. The condition of a soft plane can never be fully realized with the use of absorbent materials, which makes the geometric solution a useful alternative. As this impedance is only dependent on the geometry, the problem of the time-variance of the absorbent materials is practically solved. On the other hand, this solution is efficient only for some frequencies.

This problem can be dealt with using a barrier whose channels have different lengths, using the fork gradient shown in Figure 1(c). This corresponds to using a strip of absorbent material whose impedance changes gradually along the length of the material. The idea is similar to chirped mirrors in optics, made out of different layers that can filter different wavelengths.

For the current investigation, a 2D BEM analysis has been performed, assuming the invariance of the system on the y-axis. OpenBEM, an open-source software developed in the Matlab environment by the University of Southern Denmark [11], has been used. OpenBEM solves the Helmholtz equation using a direct collocation approach.

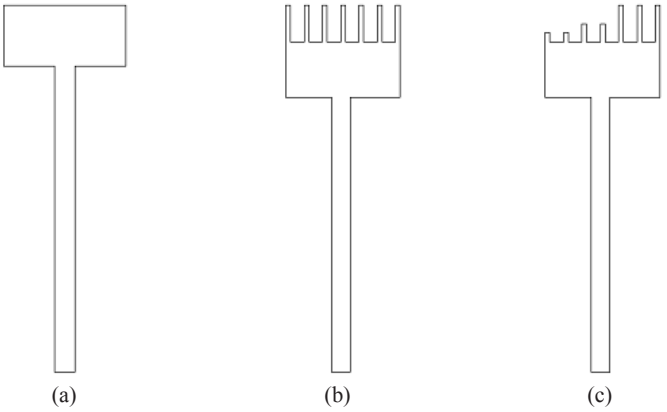

Figure 1. Different barriers used for the simulation corresponding to (a) T-shape, (b) fork shape, (c) fork gradient

The set-up for the simulation is shown in Figure 2. In the numerical model, the ground is assumed to be perfectly reflecting. The source is placed on the ground, in order to prevent unwanted reflections, and at 8 m distance from the barrier. On the other side of the barrier, 9 microphones are placed in a regular grid structure, at the different heights of 0, 1.5 m and 3 m from the ground, and at the distances 20, 50, 100 m from the barrier. Simulations are performed at the middle frequencies of the one-third octave bands. Simulations are initially performed without barrier, then with the three different barriers shown in Figure 1 and with a normal barrier of the same height and without added devices. Similar simulations have also been performed in the presence of absorbent materials.

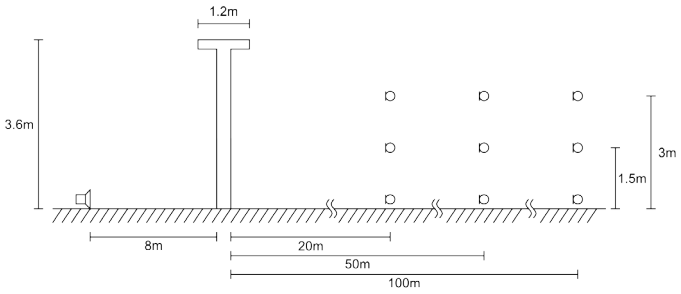

Figure 2. The simplified set-up of the BEM simulations

It is possible to add material properties in the OpenBEM software. The method used in the simulations follows the semi-empirical law of Delany and Bazley [12]. Allard and Champoux [13] derived the following empirical formulae

$$k = \left(\frac{\omega}{c}\right)[1 + 0.0978X^{-0.7} + i0.189X^{-0.595}] \quad (2)$$

$$Z_c = 1 + 0.00571X^{-0.754} + i0.087X^{-0.732} \quad (3)$$

where $X = \rho_0 f / R_s$, ρ_0 is the density of air, R_s is the flow resistivity, f is the frequency and Z_c is the normal surface impedance [13]. This semi-empirical model, drawn from the best fits of a large number of impedance tube measurements, is valid for $0.01 < X < 1.0$. In the simulations, a flow resistivity of 30000 Ns/m^4 was used, which is a good description for mineral wool applied to the noise barrier and well within the values of validity of Eqs. (2) and (3).

The insertion loss (IL) in dB is calculated as an average value for the 9 points, according to the formula

$$IL = -10\log_{10}(R) \quad (4)$$

$$R = \frac{1}{n}\sum_{i=1}^{n}\left(\frac{p_i}{\bar{p}_i}\right)^2 \quad (5)$$

where p_i represents the pressure on the i^{th} microphone and $\bar{p}_i$ the pressure on the i^{th} microphone position of the configuration without a barrier.

RESULTS

The results of the insertion loss for the various barrier designs corresponding to a straight barrier, T-shape, fork shape and fork gradient barrier are shown in Figure 3. The improvement of the IL using the fork shape and fork gradient barriers compared to the straight and T-shaped barriers can be seen in Figure 3. At some frequencies, an improvement of up to 10 dB for the fork shape can be found. A decrease in IL at around 500 Hz for the fork shape can be observed and corresponds to the maximum of the impedance. According to Eq. (1), the maximum IL is expected when $kd = \pi/2$, which for d = 400 mm, occurs at the frequency f = 210 Hz. The results for the fork shaped barrier also shows peak IL between 600 and 800 Hz.

The use of the fork gradient barrier, where channels of different depths are used, presents an input impedance that changes along the length. It represents a considerable improvement in the insertion loss as the attenuation is better distributed along the considered frequency range, as shown in Figure 3. The IL at 500 Hz has increased by around 5 dB for the fork gradient barrier compared to the fork shaped barrier.

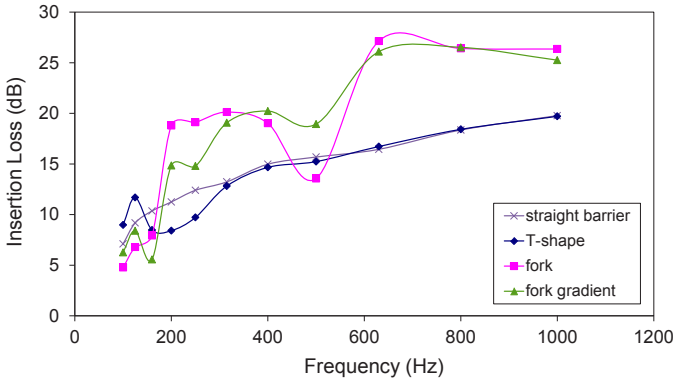

Figure 3. Insertion loss for the various barrier designs corresponding to a T-shape, fork-shape, fork gradient and a straight barrier

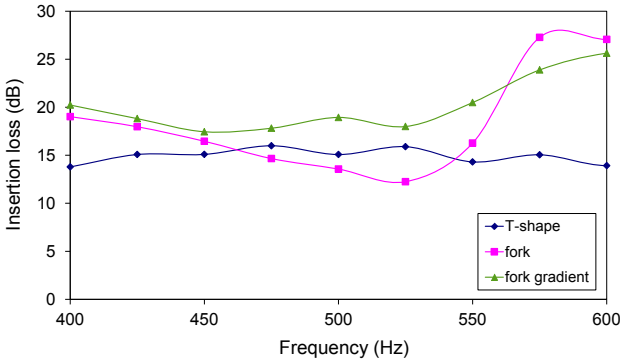

Figure 4. Insertion loss for a narrow band frequency range from 400 to 600 Hz

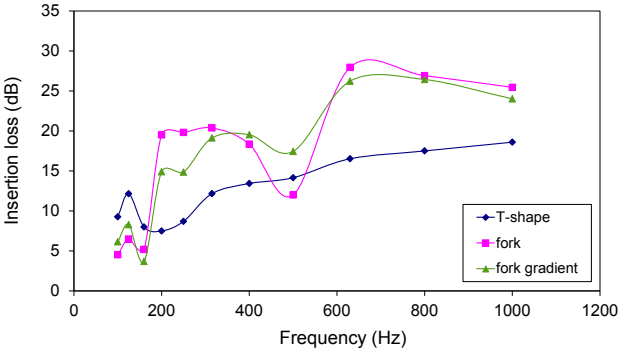

(a)

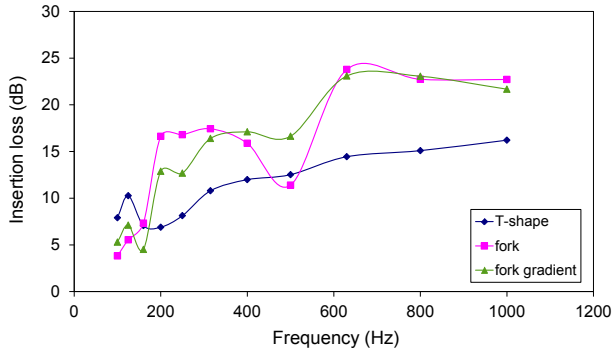

(b)

Figure 5. Insertion loss at two different receiver points on the ground at (a) 20 m and (b) 100 m from the barrier

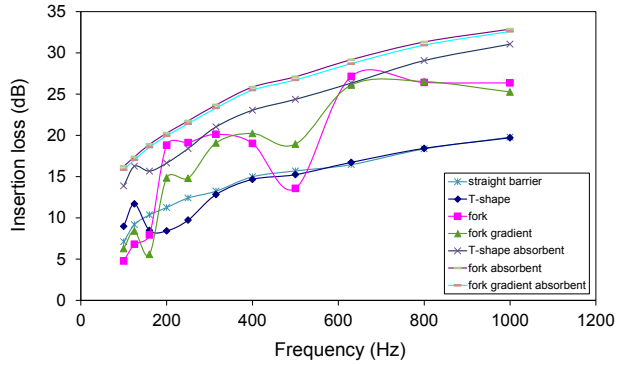

Figure 6. Insertion loss for the various barrier designs with and without mineral wool

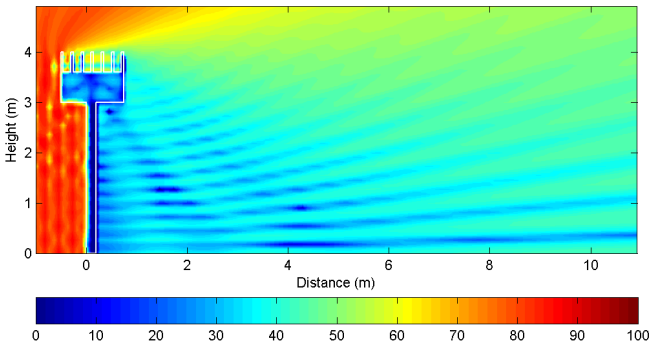

(a)

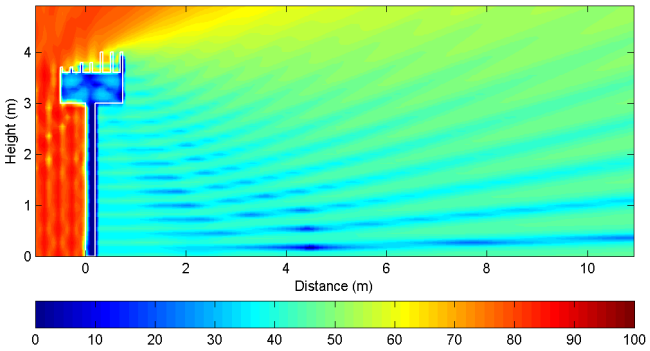

(b)

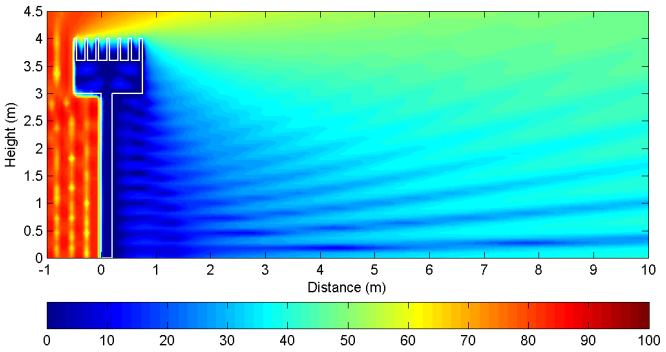

(c)

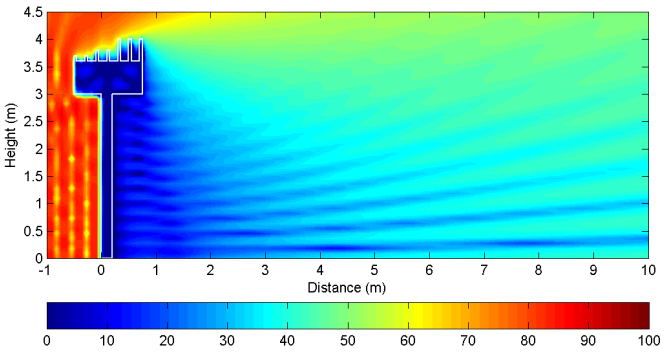

(d)

Figure 7. Sound pressure level at a frequency of 630Hz for (a) the fork barrier without absorbent material, (b) the fork gradient barrier without absorbent material, (c) the fork barrier with absorbent material, and (d) the fork gradient barrier with absorbent material

It is of interest to observe the insertion loss for the various barrier designs in a narrower frequency range corresponding to frequencies between 400 Hz and 600 Hz. In order to achieve better accuracy, simulations have been performed at increase frequency resolution. From Figure 4 it is clear that the *IL* related to the fork barrier is smooth and the dip in *IL* is broad. The same applies to a higher degree for the fork gradient barrier.

An average value of the insertion loss for the 9 microphones positions was calculated in order to represent an arbitrary point in the far field. In Figure 5, two graphs are shown that correspond to the points on the ground, one at 20 m and one at 100 m from the barrier. The average insertion loss given by Eqs. (4) and (5) is a good representation of the single location, as the behaviour is very similar to the results shown in Figure 3.

In Figure 6, simulation results are presented for the case where mineral wool is covering the T-shape, fork shape and fork gradient barriers. The presence of the mineral wool consistently improves the efficiency of the barrier, as can be seen by comparing the insertion loss of the T-shape barrier with and without the absorbent wool. For the fork shape and fork gradient barriers, applying the mineral wool results in an increase in insertion loss as well as a flattening of the insertion loss over the considered frequency range. Figure 6 shows that the best performance of the barrier occurs by both modifying the geometrical shape and applying the absorbent wool. Even if clogging deteriorates the absorbent properties of the mineral wool, the geometrical properties still remain for a long-lasting performance.

The sound pressure level (SPL) at a frequency of 630Hz is presented in Figure 7 for the fork shaped barrier and the fork gradient barrier, with and without the presence of absorbent material. On the edge of the barrier, the formation of the soft plane is clearly visible. According to Eq. (1), the soft plane is expected at about 630 Hz. In the case of absorbent barriers, the frequency behaviour is flat and no soft plane can be observed.

TUNABILITY

The geometrical profile of the top of the noise barrier can be used to tune the barrier. From Eq. (1), it is observed that changing the depth d gives rise to a shift in the frequencies where maximum absorption takes place. To investigate the effect of the depth, further simulations with the shapes illustrated in Figure 8 have been performed.

The first shape h_1 has a depth d of 100 mm. From Eq. (1), the first maximum absorbance for the top layer which corresponds to $Z_{in} = 0$ is expected at $kd = \pi/2$. This occurs at a frequency of $f_0 = 840$ Hz. By doubling the comb depth d for profile h_2, an absorption peak at 420 Hz occurs. Interestingly, the frequency f_0 which is a maximum of the absorbance for h_1 corresponds to a minimum of the absorbance for h_2, which means that for h_2 most of the radiation will be reflected. A doubling of the depth d results in opposite behaviour of the two barriers in the considered frequency range. At frequencies corresponding to peak *IL* for h_1 there is minimum *IL* for h_2 and vice-versa. Hence, the insertion loss spectrum for h_2 represents the mirrored image of the same spectrum of h_1. A similar situation is expected for h_2 and h_4, h_3 and h_6, for which a doubling of comb depth d also occurs.

In Figure 9, maximum insertion loss for barrier h_1

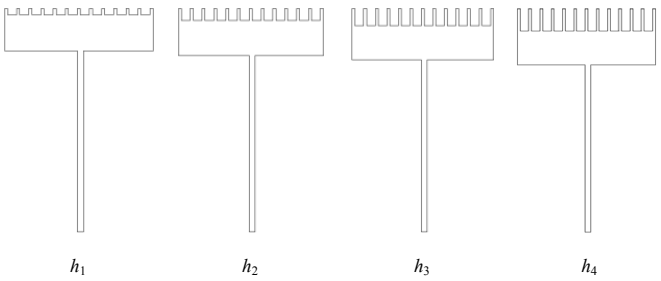

Figure 8. Fork shape barriers of different depths used for the tunability simulations

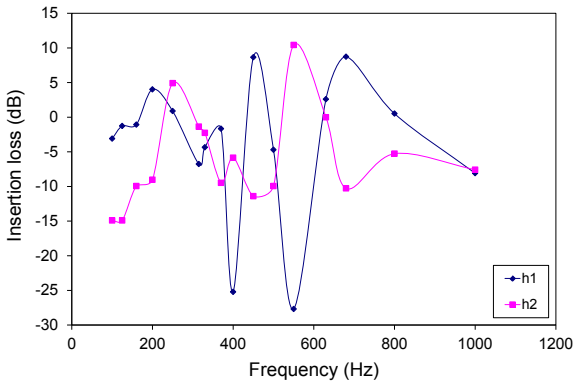

Figure 9. Insertion loss for barriers h_1 and h_2

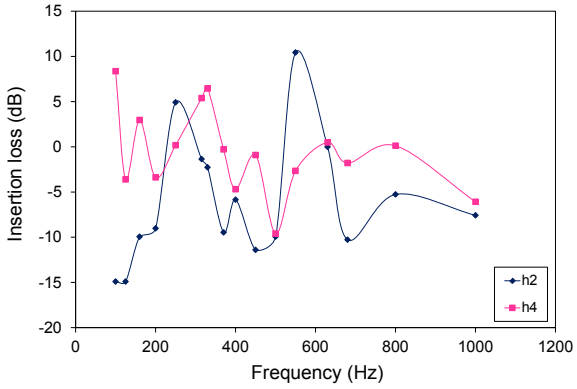

(a)

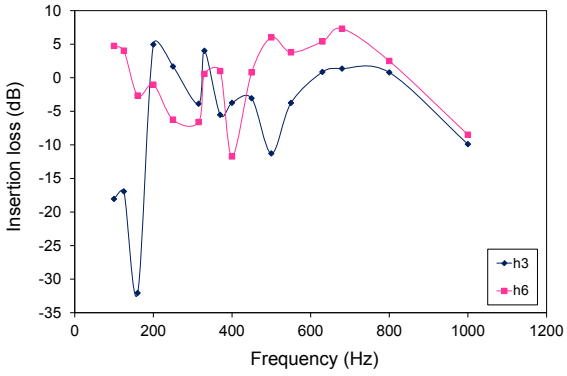

(b)

Figure 10. Insertion loss for barriers (a) h_2 and h_4 and (b) h_3 and h_6

occurs at around 680 Hz, while minimum insertion loss corresponding to $kd = \pi$ should occur at around 420 Hz. In reality the minimum is at about 550 Hz, showing that the Eq. (1) is only an approximation. A real part corresponding to $Z_{in} = i\cot(kd) + r_s$ is also present. As expected from the previous discussion, h_2 presents a mirrored behaviour compared to h_1. Similar behaviour for barriers h_2 and h_4 as well as for barriers h_3 and h_6 occurs, as shown in Figure 10. However, the effect is less clear, probably because the longer length of the channels imply more viscous effects [6].

CONCLUSIONS

Non-standard noise barriers for optimal far-field shielding have been investigated. A purely geometrical solution is not as prone to deterioration as absorbent barriers that tend to change their acoustic properties with time. The results of a two-dimensional BEM analysis for a fork shaped barrier and a fork gradient barrier are encouraging, as they present an increased insertion loss in the shadow zone of the barrier. A combination of a geometrically optimized shape with absorbent materials further increases the barrier performance.

By changing the depth of the channels in the fork shape barrier, the barrier can be tuned to further improve the barrier performance. If a mechanism is included into the barrier so that the height of the channels can be changed, this gives the possibility to change the spectral profile of the insertion loss. This could be useful in building sustainable barriers, in view of expected but not yet quantifiable shifts of the traffic noise spectrum in the future, as for example due to the increasing number of e-cars on the main transportation routes.

ACKNOWLEDGEMENT

The authors acknowledge Vicente Cutanda Henríquez for his help and support in working with OpenBEM.

REFERENCES

[1] J.P. Clairbois, J. Beaumont, M. Garai and G. Schupp, "A new in situ method for the acoustic performance of road traffic noise reducing devices", *Journal of the Acoustical Society of America* **103**, 2801 (1998)

[2] European Standard EN 1793-1 *Road traffic noise reducing devices – Test method for determining the acoustic performance, Part 1: Intrinsic characteristics of sound absorption*, 1997

[3] European Standard EN 1793-2 *Road traffic noise reducing devices – Test method for determining the acoustic performance, Part 2: Intrinsic characteristics of airborne sound insulation*, 1997

[4] R. Seznec, "Diffraction of sound around barriers: use of boundary elements technique". *Journal of Sound and Vibration* **73**, 195-209 (1980)

[5] K. Fujiwara, D. Hothersall and C. Kim, Noise barriers with reactive surfaces, *Applied Acoustics* **53**, 255-272 (1997)

[6] T. Ishizuka and K. Fujiwara, "Performance of noise barriers with various edge shapes and acoustical conditions", *Applied Acoustics* **65**, 125-141 (2004)

[7] S. Gasparoni, M. Haider, M. Conter, R. Wehr and S. Breuss, "BEM simulations of noise barriers", *Proceedings of the 39th International Congress on Noise Control Engineering, Inter-Noise 2010*, Lisbon, Portugal, 13-16 June 2010

[8] S. Gasparoni, M. Haider, M. Conter and R. Wehr, BEM simulations of diffraction-optimized noise barriers, *Boundary Elements and other Mesh reduction methods*, XXXIII, **52**, WIT press, New Forest, 2011

[9] M. Baulac, J. Defrance and P. Jean, "Optimisation with genetic algorithm of the acoustic performance of T-shaped noise barriers with a reactive top surface", *Applied Acoustics* **69**, 332–342 (2008)

[10] S. Gasparoni, M. Haider, M. Conter and R. Wehr, "BEM simulations of non-standard noise barriers with a focus on tunability", *AIP Conference Proceedings*, **1389**, pp. 460-464, Halkidiki, Greece, 19-25 September 2011

[11] V.C. Henríquez and P.M. Juhl, "OpenBEM – An open source Boundary Element Method software in Acoustics", *Proceedings of the 39th International Congress on Noise Control Engineering, Inter-Noise 2010*, Lisbon, Portugal, 13-16 June 2010

[12] M.E. Delany and E.N. Bazley, "Acoustical properties of fibrous absorbent materials", *Applied Acoustics* **3**, 105-116 (1970)

[13] J.-F. Allard and Y. Champoux, "New empirical equations for sound propagation in rigid frame fibrous materials", *Journal of the Acoustical Society of America* **91**, 3346-3353 (1992)